

In Situ Liquid Crystal Gel as a New Ophthalmic Drug Delivery System for Pilocarpine Nitrate: Improving Preocular Retention and Ocular Bioavailability

Wenqing Wu

Anhui University of Traditional Chinese Medicine

Wenxuan Cao

Anhui University of Traditional Chinese Medicine

Ye Cai

Anhui University of Traditional Chinese Medicine

Menghe Zhang

Anhui University of Traditional Chinese Medicine

Tiantian Chen

Anhui University of Traditional Chinese Medicine

Nannan Zhang

Anhui University of Traditional Chinese Medicine

Mengzhen Wang

Anhui University of Traditional Chinese Medicine

Lin Chu

Anhui University of Traditional Chinese Medicine

xiaoqin Chu (✉ XiaoqinChu113@163.com)

Anhui University of Traditional Chinese Medicine

Research Article

Keywords: Pilocarpine nitrate, Liquid crystal gel, Ophthalmic administration, Corneal penetration, Glaucoma

Posted Date: July 26th, 2021

DOI: <https://doi.org/10.21203/rs.3.rs-644389/v1>

License:  This work is licensed under a Creative Commons Attribution 4.0 International License.

[Read Full License](#)

1 **In situ liquid crystal gel as a new ophthalmic drug delivery**
2 **system for pilocarpine nitrate: improving preocular retention and**
3 **ocular bioavailability**

4 Running title: Application of in-situ liquid crystal gel in ocular drug delivery

5 Wenqing Wu^{a#}, Wenxuan Cao^a, Ye Cai^a, Menghe Zhang^a, Tiantian Chen^a, Nannan
6 Zhang^a, Mengzhen Wang^a, Lin Chu^a, Xiaoqin Chu^{a,b*}

7 ^aSchool of Pharmacy, Anhui University of Chinese Medicine, Hefei 230012,
8 China

9 ^bInstitute of Pharmaceutics, Anhui Academy of Chinese Medicine, Hefei 230012,
10 China

11
12
13 *Correspondence to: Prof. Xiaoqin Chu. School of Pharmacy, Anhui University
14 of Chinese Medicine, No. 1, QianJiang Road, Hefei, Anhui, P. R. China. Tel: (+86)
15 0551-6812-9142, E-mail: Chuxq420@163.com.

16 [#]These authors contributed equally to this work.

17
18
19
20
21
22
23
24
25
26
27
28
29

30

31 **In situ liquid crystal gel as a new ophthalmic drug delivery system**
32 **for pilocarpine nitrate: improving preocular retention and ocular**
33 **bioavailability**

34 Abstract: The purpose of this article is to develop an in-situ liquid crystal gel that can
35 be used as a novel ocular delivery system for pilocarpine nitrate (PN). The phytantriol
36 (PT) -based in situ liquid crystal gels were prepared by a vortex method using PT,
37 PEG400, Triglyceride (TAG) and water (in the ratio of 61.15:30:3.85:5, w/w). Firstly,
38 the internal structure of the PN-loaded liquid crystal gel was characterized by
39 polarizing microscope (PLM), small-angle X-ray scattering (SAXS), differential
40 scanning calorimetry (DSC) and rheology. In vitro drug release behavior and ex vivo
41 corneal permeation were investigated. Finally, eye irritation test, preocular residence
42 time evaluation, were studied in vivo and compared with eye drops. Based on various
43 characterization techniques, it is proved that the internal structure of the gel is a
44 hexagonal phase. In vitro release results identified that PN could be released
45 continuously from HII gel over a period of 24 h. The in vitro obvious permeability
46 coefficient of HII gel was 3.19-fold ($P < 0.01$) higher than that of the eye drops.
47 Compared with eye drops, the HII gel had good bioadhesion and displayed longer
48 residence time on the eyeballs surface using fluorescent labeling technology. In
49 addition, through Corneal hydration level and eye irritation test, it is conjectured that
50 HII gel will not cause eye irritation. In short, the formulation has the advantages of
51 high efficiency, slow release and non-toxicity, and will become a promising
52 pharmaceutical strategy to improve the efficacy of glaucoma.

53 Key words: Pilocarpine nitrate, Liquid crystal gel, Ophthalmic administration,
54 Corneal penetration, Glaucoma

55

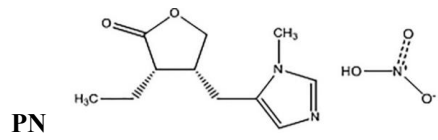
56

57

58

59 **Graphic abstract**

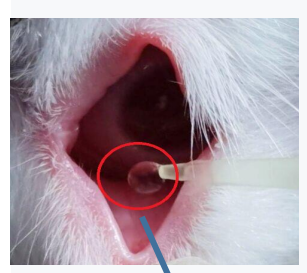
60



62

63

PN+TAG+H₂O



64 **In situ gel**

65

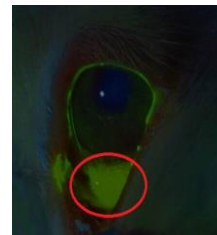
37°C

66



Pre-Corneal Residence Time

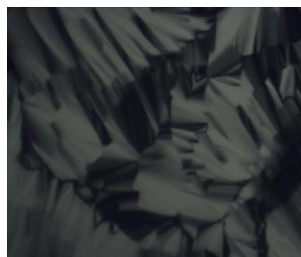
67 **Gel**



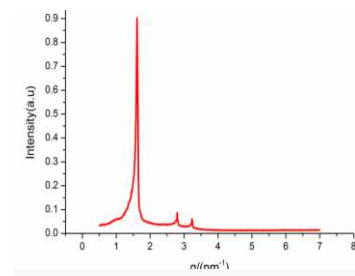
68

Characterization

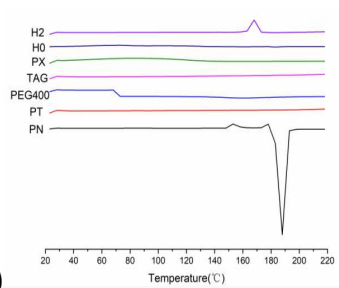
69



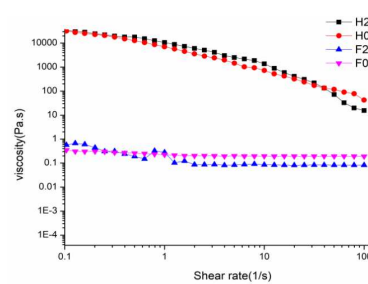
B(SAXS)



70 **A(PLM)**



D(rheology)



71 **C(DSC)**

72

73 1、 Introduction

74 Topical ophthalmic administration is the main method of ophthalmic treatment.
75 However, due to the high sensitivity of the eye and unique physiological barriers
76 (including corneal and conjunctival barriers, blood-water barriers and blood-retinal
77 barriers), the drug has low bioavailability and poor efficacy. Commonly used ocular
78 dosage forms are topical eye drops and ophthalmic ointments. However, most of the
79 liquid is discharged from the lacrimal duct after the eye drops are administered, and
80 may cause systemic toxicity after being absorbed through the nasopharynx. Due to its
81 greasy properties and blurred vision, eye ointment has poor patient compliance when
82 applied to eye ointment^[1].

83 Over these years, a growing number of innovative drug delivery systems have
84 been applied to the eyes. Such as liposome nanoparticles and microemulsion, to
85 extend the retention time of the eyes, thus reducing the frequency of medication and
86 increasing bioavailability. However, their drug delivery potential in ophthalmology is
87 limited by the rapid clearance of the anterior cornea due to the same rapid clearance
88 as the water-soluble eye drops. Therefore, considering the unique physiological
89 structure of the eye, effective ocular drug delivery still faces many challenges and
90 needs to find a more effective ocular delivery system.

91 In recent years, in-situ gel has become a new type of sustained release system^[2,3].
92 It is a precursor for administration and then transforms into a gel at the drug delivery
93 site. Compared with other ophthalmic preparations, the precursor preparation of liquid
94 crystal gel has a longer residence time in the eye and good curative effect. In
95 addition, in situ gel is in the form of ordinary solution, similar to eye drops, so the
96 drug is simple and good compliance^[4-8]. Conversion from solution to gel is usually
97 caused by some physiological or external stimuli, such as variances in pH value, ionic
98 strength or temperature between the formulation outside the body and the internal
99 tissues^[9]. When the formulation is exposed to artificial tears, the precursor solution is
100 transparent and can spontaneously become a gel. Since the triggering factor of this
101 phase change is due to the existence of the water environment, it can also be realized

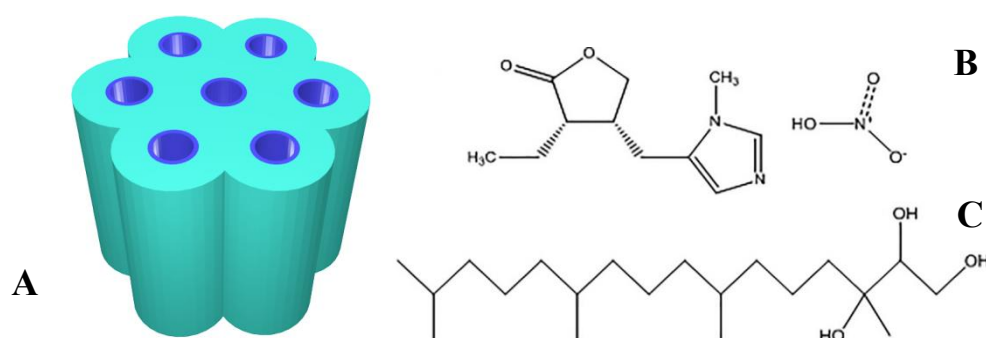
102 directly in the physiological fluid. Compared with other methods, such as ultraviolet
103 light and temperature, this method can cause phase transition^[10]more mild. According
104 to the literature, it is found that many kinds of in-situ gels have been used in eye
105 administration to improve ocular bioavailability like use of temperature-dependent
106 in-situ gelation polymer (Ploxamer)^[4-8], pH-dependent in-situ gelling polymers
107 (Carbopol and Hypromellose)^[11-13], and ionic strength-dependent in-situ gelling
108 polymer (Gellan gum). However, there are few reports on in situ liquid crystal gel for
109 ocular drug delivery.

110 An amphiphilic substance containing a hydrophilic head group and a
111 hydrophobic hydrocarbon chain domain self-assembles after adding water to form a
112 long-range ordered structure called a lyotropic liquid crystal phase^[8]. For example,
113 lamellar phase (L_α), reverse bicontinuous cubic phase (Q_{II}) and reverse bicontinuous
114 hexagonal phase (H_{II}) have received more and more attention due to their unique
115 internal frame and broad drug capacity. Among them, the hexagonal liquid crystal as a
116 drug carrier has attracted widespread interests due to its good stability, potential drug
117 slow-release ability^[14]. Phytotriol(PT) (shown in Fig.1) are generally considered safe
118 drug matrix and amphiphilic lipids with good mucosal adhesion and biocompatibility,
119 which was often utilized to form liquid crystals. The lyotropic liquid crystal delivery
120 system has many advantages, such as simple preparation, easy to use, reduced dose,
121 and sustained release effects, PT-based liquid crystal gels have been used in the
122 treatment of rheumatoid arthritis and postoperative analgesia^[15]. However, there are
123 few studies on PT in ocular delivery systems.

124 Glaucoma is one of the major public health problems in the world. This is a
125 chronic progressive eye disease caused by the apoptosis of retinal ganglion cells and
126 subsequent degeneration of nerve tissue. According to the survey, more than 70
127 million people in the world suffer from glaucoma, and about 10% of them are blind,
128 which makes it the main cause of irreversible blindness in the world2020^[16]. However,
129 this number may rise to 11.1 million by 2020. Pilocarpine nitrate is a drug that
130 directly acts on the parasympathetic nerve. It can directly stimulate muscarinic
131 receptor M of iris and ciliary body, cause the contraction of iris and ciliary body, open

132 the anterior chamber angle, promote the outflow of aqueous humor through trabecular
133 meshwork structure, and produce the effect of lowering intraocular pressure^[17]. It has
134 been used in the treatment of chronic open Angle glaucoma and acute closed Angle
135 glaucoma for more than 100 years^[18]. At the same time, PN has been used the longest
136 as a mainstay drug for glaucoma therapy, and is one of the least-expensive and the
137 most readily available medications^[19]. Applied in the eye, PN can penetrate the
138 eye wall with miosis beginning in 15-30 min which last up to 4-8 h^[20]. Due to poor
139 corneal permeability, short anterior corneal retention time and poor anterior corneal
140 tear flushing, PN eye drops need to be administered frequently, generally 3-6 times a
141 day ^[21]. Therefore, the bioavailability is extremely low (less than 5% or even less than
142 1%). At the same time, frequent daily administration can cause a series of side effects,
143 such as pupil contraction and myopia, and even a series of gastrointestinal reactions. In
144 addition, our previous research has developed a liquid crystal gel. Based on this, we
145 made the gel into a precursor to improve compliance^[22].

146
147
148
149
150
151



152
153
154
155
156

Fig. 1 The pores assemble into hexagonally packed columnar mesophases^[23] (A),
Molecular structure of PN (B) and PT (C)

157 1. Materials and methods

158 1.1 Materials

159 PT was acquired from Shanghai Aladdin Biotechnology Co., Ltd. (Shanghai,
160 China).PN was bought from Shanghai TargetMol Biotechnology Co., Ltd. (Shanghai,
161 China). Triglyceride (TAG) was bought from Sigma-Aldrich Trading Co., Ltd.
162 (Shanghai, China). PEG400 was bought Beijing Solarbio & Technology Co., Ltd
163 Ltd. (Shanghai, China).

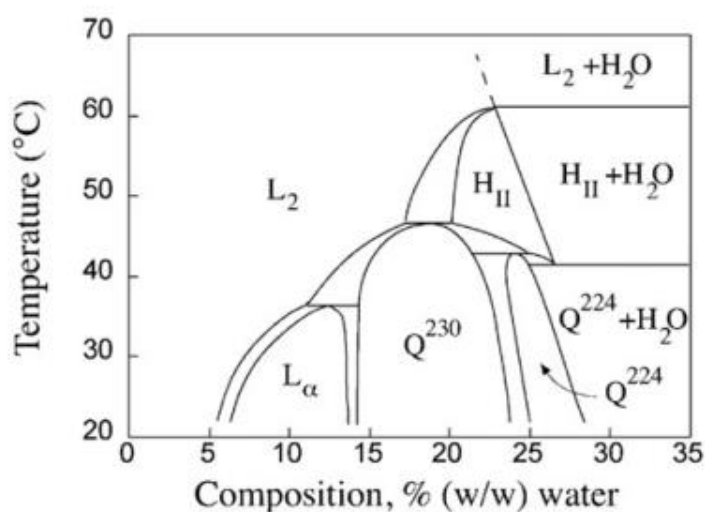
164 The weight of adult New Zealand white rabbit was in the range of 2.5-3.0 kg,
165 which is supplied by the Animal Experimental Center of Anhui University of Chinese
166 Medicine (Hefei, China). All animal experiments were performed in accordance with
167 the guidelines approved by the ethics committee of Anhui University of Chinese
168 medicine (Hefei, China)

169 2.2 Prescription Screening

170 2.2.1 Preparation

171 According to the literature^[24]and our former research (Fig.2), the formulating
172 method was as follows. Firstly, appropriate amount of PT and TAG were mixed and
173 heated to 60 ± 0.5 °C to prepare oil phase. Secondly, PN was placed in water at $60 \pm$
174 0.5 °C to prepare aqueous phase (PEG400 and water). Finally, the water phase in the
175 same temperature was added to the oil phase rapidly, and the mixture was
176 immediately rotated for 5 minutes to obtain a liquid crystal gel precursor.

177 Then, PT-TAG (oil phase) and PEG400-water (water phase) systems were used
178 to gradually change the weight ratio of the prescription from 10%: 90% to 90%: 10%.
179 The prescription was screened by the above-mentioned preparation method, and four
180 blank formulas were prepared, namely P 0, P 1, P 2 and P 3. The optimal proportion of
181 stable self-assembled liquid crystal system was determined. Considering the solubility
182 of the drug and the particularity of ophthalmic administration, three preparations were
183 made with drug contents of 0% (F0) , 0.5% (F1) , 1% (F2) and 1.5% (F3) ,
184 respectively. After 72 h of stabilization, the appearance of the preparations was
185 observed.



186

187 Fig.2 Temperature composition phase diagram of the phytantriol/water binary
188 system^[25].

189

190 2.2.2 Phase Conversion

191 2.2.2.1 The Minimum Volume (V_m) and Time (T_g) for Phase Conversion

192 In the rotor method^[26], 200 mg of the formulation is accurately weighed and
193 added to a tube with a rotor (10 mm × 6 mm). The test tube was immersed in a water
194 bath at 37 °C with a stirring speed of 30 rpm for 5 minutes. Then, 10 μL of artificial
195 tears were added to the centrifuge tube every 1 minute until the rotor was completely
196 stopped due to gelation. The time when the rotor stops moving due to gelation is
197 determined as T_g , and the total volume of water added at this time is determined as
198 V_m .

199 2.2.2.2 Determination of the gelling capacity

200 In order to simulate the gelation ability in the human environment, the precursors
201 were placed in a centrifuge tube containing 2 mL fresh simulated tears (pH 7.4,
202 37±1 °C) to determine the gelling ability, the time taken for its gelling formation then
203 dissolution of the gels were visually observed and the gelling capacity were
204 evaluated^[27] as follows:

205

(-)	No gelation
(+)	The gel formed after few minutes and dissolved rapidly
(++)	Immediate gelation and remains for few hours
(++ +)	Immediate stiff gelation which remains for extended period of time

206

207 2.2.3 Determination of the pH and osmotic pressure

208 pH was measured at 25 °C by a Model PHS-3C pH-meter (Shanghai Precision
 209 Scientific Instrument Co., Ltd). The freezing point method of a Model FM-9X
 210 Osmometer (Shanghai Precision Scientific Instrument Co., Ltd) was used to evaluate
 211 the osmotic pressure.

212 2.3 Characterization of structure

213 2.3.1 PLM

214 Polarized light microscope observes the internal structure of the precursor and
 215 the liquid crystal gels (CK-500, Shanghai Caikon Optical Instrument Co., Ltd.
 216 Shanghai, China)^[28]. Observed by PLM, the isotropic liquid and Q_{II} have no
 217 birefringence, and the background is dark. The characteristic of L_α and H_{II} is a
 218 birefringent structure, that is, H_{II} has a fan-shaped structure. Greasy streak texture or
 219 Maltese cross shape can be observed in the L_α phase^[29].

220 2.3.2 SAXS

221 Further structure analysis and phase identification of LC gels were carried out by
 222 SAXS measurement (Anton Paar, Graz, Austria) at room temperature. The specimen
 223 were tested at 40 kV and 50 mA for 10 min using an X-ray source (Cu K_α radiation,
 224 λ=0.154 nm). After the sample was equilibrated for 10 min, the scattering pattern was
 225 collected, and the scattering intensity was plotted against the q value, which enabled
 226 the identification of the peak position. The type of liquid crystal was determined by
 227 the peak scattering vector ratio^[30].

228 The relevant parameters of the liquid crystal structure are calculated by the
 229 following formulas^[31]:

230
$$q = (4\pi \sin\theta) / \lambda$$

231 $d=2\pi/q$

232 $\alpha = (h^2 + k^2 + l^2)^{1/2}d$

233 Where θ is the scattering angle, q is the position of the first peak, k is the
234 wavelength of 0.154 nm, d is the distance between the reflecting interplanar space of
235 the liquid crystalline phase, α is the LP which indicates the size of aqueous channels
236 in the LC internal structure, and h , k , and l are the Miller indices and have no
237 dimension.

238 2.3.3 DSC

239 DSC is used to evaluate temperature and enthalpies of phase transitions during
240 melting and crystallization^[32]. 5 to 15 mg samples (PN, PT, TAG, PEG400, Physical
241 mixture of PT, PEG400, PN, TAG, Blank in situ liquid crystal and drug loaded in situ
242 liquid crystal gel) were weighed by Mettler M3 microbalance in a standard 40 μ L
243 aluminum pot and sealed immediately. The scanning speed was 10 $^{\circ}$ C/min. The
244 scanning range was 20-220 $^{\circ}$ C. The atmosphere was nitrogen (flow rate was 20
245 mL/min), an empty pot is used as a reference. The instrument determines the melting
246 temperature of the solid components and the total heat transferred during any
247 observed thermal process.

248 2.3.4 Rheological characterization

249 A DHR-2 rheometer (TA Instruments, New Castle, DE) was used to evaluate the
250 rheological characteristics of LC gels and incorporate a cone-plate sensor with a cone
251 angle of 1 $^{\circ}$ and a diameter of 20 mm. In the rheological test, the flow rate of the liquid
252 crystal gel was studied by controlling the shear rate from 1 to 100 s^{-1} during the
253 experiment, and the temperature was maintained at $37 \pm 2^{\circ}$ C. Meanwhile, frequency
254 scanning was used to further evaluate the rheological behavior of the preparation.
255 Finally, a temperature scan was used to study the viscosity change with increasing
256 temperature, and the temperature setting range was 25~45 $^{\circ}$ C.

257

258 3.3 Evaluation of in vitro properties

259 3.3.1 In vitro release study

260 The in vitro release of PN from liquid crystal was studied by dynamic dialysis^[33].
261 In short, 50 mg fresh PN liquid crystal gels were transferred into dialysis bags
262 (MWCO 8KD-14KD Aladdin,USA) to meet the dialytic capacity of the drug. 150 μ
263 L of eye drops were used as a control. Both eye drops and PN liquid crystal gel
264 contain 1.5 mg of PN. Then, the dialysis bag was immersed in 12 mL of artificial tears
265 at 37 ± 1 °C under agitation at 100 rpm.

266 At predetermined time intervals, 1 ml samples were taken at 0.17, 0.5, 1.00, 1.50,
267 2.00, 4.00, 8.00, 12.00, 24 h. Simultaneously, the STF of the same volume was
268 replaced. The samples were filtered by 0.45 μ m microporous membrane, and the
269 drug content was determined by HPLC. The cumulative release percentage (%) was
270 plotted against the time (T, h). The cumulative drug release (Q_n, μ g / mL) was
271 calculated by the following formula:

$$Q_n = c_n \times v_0 + \sum_{i=1}^{n-1} c_i \times v_i$$

272 C_n represents the concentration of PN at each sampling time. V₀ stand for the
273 volumes of the dissolution medium. V_i represents sample volume. C_i represents the
274 PN concentration of the ith sample.

275 The dynamics and mechanisms of PN release in the gel were evaluated by fitting
276 the zero order, first order, Higuchi equation and Ritger-Peppas model to evaluate the
277 dynamic model with the highest correlation coefficient. The release kinetics and
278 mechanism of liquid crystal gel were fitted by the following formula:

279 Zero order model equation: $y = k_1t + a_1$

280 First order model equation: $\ln(100 - y) = k_2t + a_2$

281 Higuchi equation: $y = k_3t^{0.5} + a_3$

282 Ritger peppas model equation: $y = k_4t^n$

283 In the above formulas, y is the cumulative release percentage. t is the sampling
284 time; K₁, K₂, K₃ and K₄ are the release rate constants of the equation; a₁, a₂ and a₃ are
285 constants; and n is the release index describing the release mechanism.

286 3.3.2 In vitro corneal permeability study

287 Remove the eyeballs of New Zealand rabbits that have been derived, and
288 immediately remove the cornea into glutathione bicarbonate ringer(GBR) buffer. The
289 modified Franz diffusion cell was used for in vitro corneal penetration studies, and the
290 effective diffusion area was 0.5024cm². Then, the corneas were fixed between the
291 receptor and the donor compartments with the epithelial side facing the donor
292 chamber. Each formulation (50 mg) with concentration of 1.50 mg PN was transferred
293 to the donor compartment, and then the receptor chamber was introduced into 5 mL
294 GBR solution pre-adjusted to a temperature of 37 °C. Simultaneously, 100 μ L PN
295 eye drops (containing 1.50 mg PN)was used as the control group. The samples (0.4
296 mL) were collected at specified intervals (30, 60, 90, 120, 180, 240, 300 and 360 min)
297 and replaced with fresh GBR of the same volume^[34]. The corneal penetration test for
298 each formulation was repeated three times. The samples were filtered by 0.22 μm
299 microporous membrane. The PN concentration of samples was determined by HPLC
300 as described above with correction for the volume replacement. The amount of PN
301 that permeated the corneal epithelium was plotted versus time and the slope of the
302 linear portion of the graph was calculated. The steady-state flux [J_{ss} , μg/(cm²·s)] and
303 apparent permeability coefficient (P_{app} , cm/s) were determined as follows:

304

305

306

307

$$J_{ss}=C_0 * P_{app}$$

$$P_{app} = \frac{\Delta Q}{\Delta t \cdot C_0 \cdot A \cdot 60}$$

308 $\Delta Q/\Delta t$ represents the slope of the linear part of the drug content (Qn/μg) in the
309 receiving pool versus time; C_0 represents the initial concentration of the drug in the
310 donor cell (g/mL). A represents the corneal surface area (0.5024cm² in this study), and
311 60 is the factor used to convert minutes into seconds.

312 3.3.3 Corneal hydration level

313 In order to evaluate the irritation of the preparation on the cornea, the corneal
314 hydration level (HL) was measured after in vitro corneal permeability test. At the end

315 of the in vitro penetration study, each cornea was rinsed with normal saline to remove
 316 the residual preparation on the corneal surface, and then weighed. Then, after drying
 317 at 70 ± 0.5 °C for 12 h, the sample were weighed. In general, The HL value of
 318 healthy cornea was 76~80%, corneal hydration value of more than 83% indicates
 319 some degree of corneal injury^[35]. The HL% value was calculated using the following
 320 equation^[36]:

$$321 \quad HL\% = \frac{W_t - W_d}{W_t} \times 100$$

322 3.4 In vivo performance evaluation

323 3.4.1 In vivo eye irritation studies

324 The potential ocular irritancy and/or damaging effects of the formulations
 325 components and eye drops were evaluated according to a modified Draize test on
 326 male New Zealand albino rabbits (n = 6)^[37]. All rabbits were randomly divided into
 327 two groups with three rabbits in each group, In the single dose trial, all samples
 328 were dripped into the inferior conjunctival sac of each rabbit's right eyes, the left eyes
 329 of the contralateral side were treated with saline. After administration, gently close the
 330 eyelids for about 10 seconds to avoid loss of preparation. Observe eye reactions
 331 (redness, swelling, conjunctival edema, iris and corneal damage, etc.) at 5, 15, 30
 332 minutes and 1, 2, 3, 5, 9, 12, and 24 hours after administration. In the multiple
 333 administration test, the eye tissue reaction was observed after 1, 2, 3, 4, 5, 6, 7 days
 334 according to the method of single administration. Then, according to the evaluation
 335 criteria in Table 1, the irritation of the samples to the eyes were judged.

336 Table 1. Classification of eye irritation

337	Score	Stimulus level
338	0–3	Nonirritant
339	4–8	Slight irritation
340	9–12	Medium irritant
341	13–16	Severe irritation

342

343 3.4.2 Pre-Corneal Residence Time Analysis

344 In this experiment, sodium fluorescein-loaded formulations (i.e. LC gels and
345 solution) were prepared to evaluate their in vivo preocular residence according to a
346 previously reported protocol. Generally, 1% sodium fluorescein was used to replace
347 PN in the preparation, and then the preparation containing sodium fluorescein was
348 prepared by the same method as the liquid crystal gel precursor. Then, 50 mg of the
349 precursor preparation and 50 μ L of fluorescein sodium solution were dropped on the
350 lower dome of the rabbit eyes, and finally, the fluorescence intensity was monitored
351 with a fluorescent lamp and excited with blue-light-activated fluorescent lamp.

352 3 Results

353 3.1 Prescription screening

354 3.1.1 Screening and optimization of prescription

355 In 2003, Barauskas and Landh reported the phase diagram of PYT/water binary
356 system^[38]. In addition, we fully considered the solubility of PN and the basis of our
357 previous work in selecting the formula ratio, and prepared four blank liquid crystal gel
358 precursors (P0, P1, P2, P3). The above samples need to be balanced at room
359 temperature for 72 h, and then the appearance of the samples can be observed by
360 naked eyes under good light conditions. As shown in Table 2. P1 (PT: PEG: TAG:
361 water = 61.15: 30: 3.85: 5) has better fluidity and better transparent appearance than
362 other preparations. Therefore, considering the solubility of PN, the preparation
363 contains 0.5% (F1), 1% (F2), 1.5% (F3) PN drug-loaded preparation.

364

365 **Table 2 Formulation and drug loading screening of in situ hexagonal liquid crystal**

Formulations	PT(wt%)	PEG400(wt %)	TAG(wt%)	Water(wt%)	PN(wt%)	Appearance
P0	61.15	32.50	3.85	2.50	0	Milky

P1	61.15	30.0	3.85	5.00	0	Clarify, Good liquidity
P2	61.15	27.5	3.85	7.50	0	Milky, Poor liquidity
P3	61.15	25.00	3.85	10.00	0	Milky, Poor liquidity
F0	61.15	30.00	3.85	5.00	0	Clarify, Good liquidity
F1	61.15	30.00	3.85	5.00	0.50	Clarify, Good liquidity
F2	61.15	30.00	3.85	5.00	1.00	Clarify, Good liquidity
F3	61.15	30.0	3.85	5.00	1.50	Milky, Poor liquidity

366

367 3.1.2 The Minimum Volume (V_m) and Time (T_g) for Phase Conversion

368 The appearance before and after phase inversion was shown in Fig.3. When the
369 liquid crystal precursor was exposed to artificial tears, it undergoes a phase change
370 due to the presence of an aqueous environment, and the precursor solution gradually
371 becomes a gel state. Experimental results showed that 80 μL of artificial tears need to
372 be added to 200 mg of the precursor preparation to make the phase change into a gel
373 state, and the time required is about 1.5 to 2 second

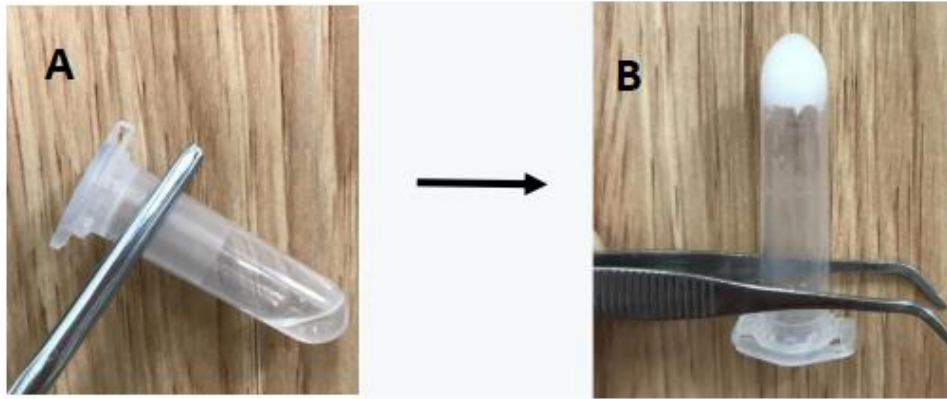


Fig3. In situ liquid crystal gel before(A) and after steering(B)

374

375

376 3.1.3 Determination of the gelling capacity

377 It was observed that the best prescription P1 showed the "+ +" grade of gelation
 378 ability, which is reported to be the most satisfactory grade^[27]. The precursor
 379 formulation was gelatinization immediately after exposure to PN at 37 °C degrees
 380 can remain for a long time.

381 3.2 Characterization of preparations

382 3.2.1 PLM

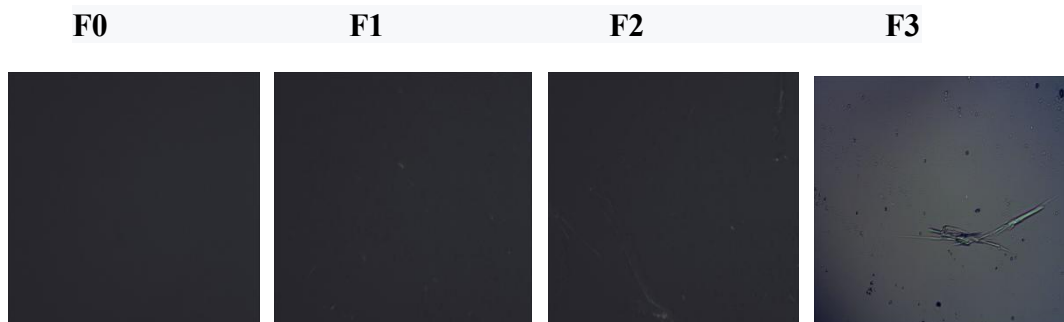
383 We put the samples under the PLM for observation. The precursor
 384 formulations(F0,F1,F2,F3) showed a black background under PLM, the liquid crystal
 385 gel(H0,H1,H2,H3) formed after phase inversion had a clear fan-shaped texture-like
 386 optical birefringence structure observed under PLM, and it can be confirmed that it is
 387 a hexagonal phase liquid crystal. H0, H1 and H2 had no drug crystals, while H3
 388 showed a few crystals (as shown in Fig 4).

389

390

391

392



393

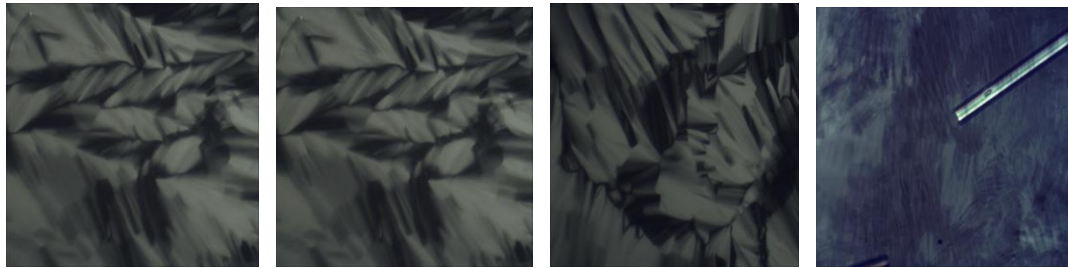
394

H0

H1

H2

H3



395

396

397

398

399

Fig. 4. Observe precursor formulations and liquid crystal gels under PLM (magnification $\times 100$)

3.2.2 SAXS

400

401

402

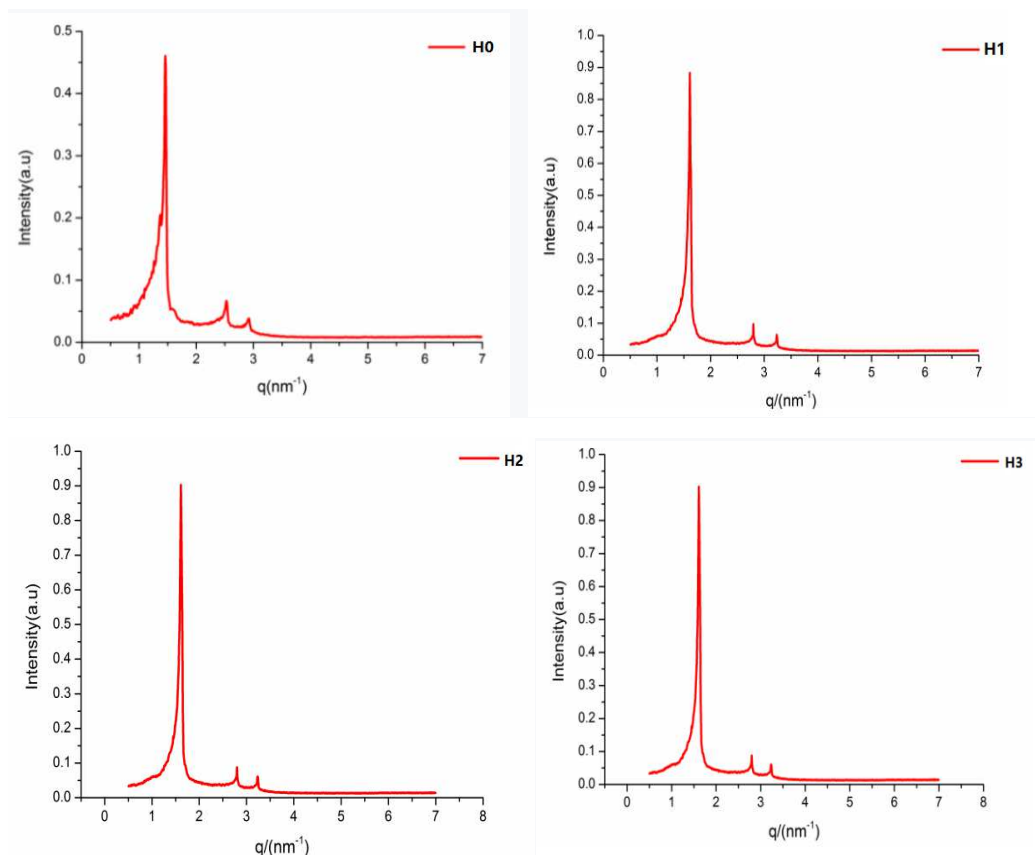
403

404

405

In order to further confirm the composition of the gels containing PN, SAXS technique was carried out in this paper. The structures of the gels could be determined according to the ratio of the q corresponding to scattering peaks in the SAXS curves. The typical SAXS pattern was displayed in Fig 5, with respective relative ratios of gels as $1:\sqrt{2}:\sqrt{3}$. The results showed that the liquid crystal gels formed after the precursor phase inversion were hexagonal liquid crystal gels.

406



407

408

409

Fig.5 Small-angle X-ray diffraction detection diagram of in situ liquid crystal

410

Table 3. Lattice Parameters (α) and Layer Spacing (d) of liquid crystal gel

Formulations	Space group	Bragg peaks	α (\AA^*)	d (\AA)
H0	H _{II}	1: $\sqrt{2}$: $\sqrt{3}$	47.95	41.52
H1	H _{II}	1: $\sqrt{2}$: $\sqrt{3}$	48.16	41.71
H2	H _{II}	1: $\sqrt{2}$: $\sqrt{3}$	48.58	42.07
H3	H _{II}	1: $\sqrt{2}$: $\sqrt{3}$	47.32	40.98

411

* 1 \AA = 10^{-10}m

412

Distinctly, the content of PN may affect the internal symmetry of gels mesophases due to the alterations of the lattice parameter. When PN was added to the formulation, the lattice parameter changed from 47.95 \AA to 48.58 \AA . These results could prove that the hydrophilic PN were mainly contained in the water channel, and minimally contained in the lipid-water interface. According to literature research, this may be due to the partial hydration of the polar head group and water in the lyotropic liquid crystal system, which leads to the expansion of the hydrophilic head group of PT^[39]. However, the decrease in the value of α in H3 may be due to the dehydration of the polar head group of PT. When the hydrophilic PN binds more water molecules, it will cause the hydrogen bond between the PT head group and water to decrease, that is, the effective size of the PT head group decreases and the α value decreases^[40].

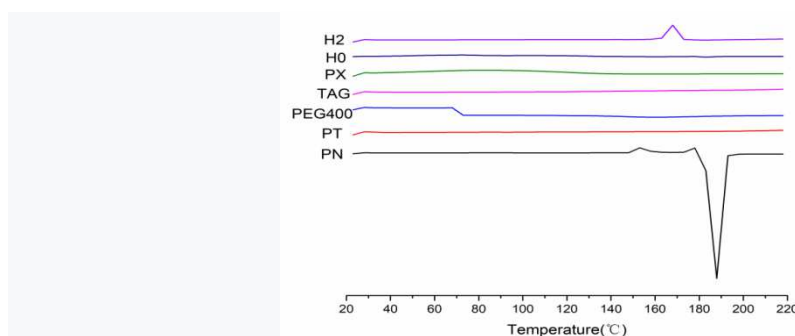
423

3.2.3 DSC

424

As shown in Fig.7, the thermograms showed a sharp endothermic peak at 190 $^{\circ}\text{C}$, which corresponded to the melting point of PN in the crystal form. However, the endothermic peaks of PN completely disappeared in the thermograms of PX (Physical mixture) and H3. At the same time, it can be seen from the figure that the melting point of H3 was 165 $^{\circ}\text{C}$.

428



429

430

Fig.6. DSC thermograms

431 3.2.4 Rheological characterization

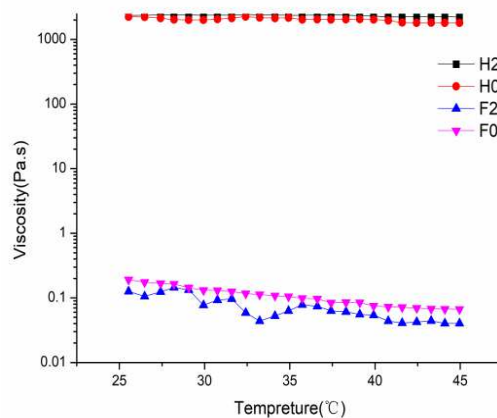
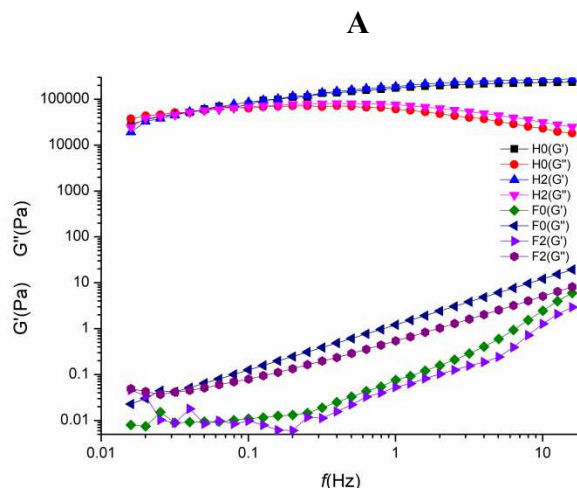
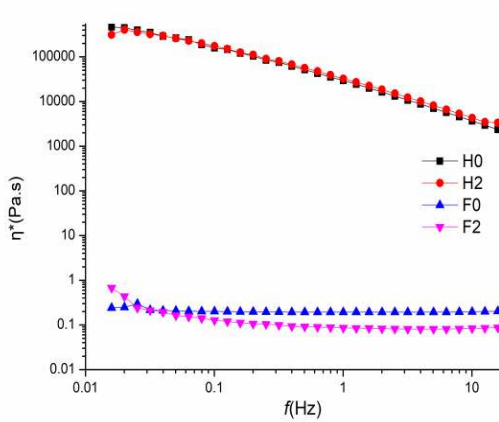
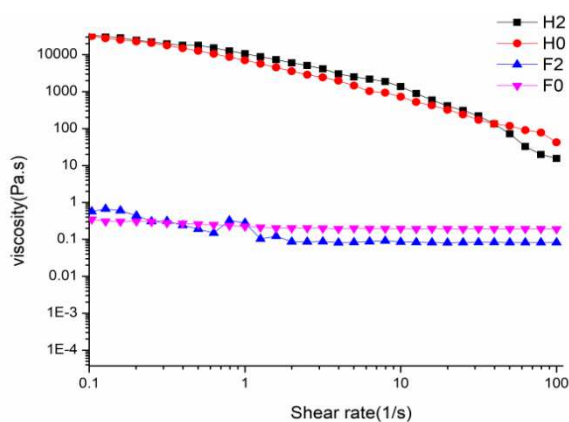
432 It could be seen from the rheological curve of Figure 7(A) that as the shear rate
433 increases, the viscosity of the precursor formulation gradually stabilizes. Obviously,
434 the viscosity of F2 is lower than F0, so the drug can improve the fluidity of the liquid
435 crystal gel precursor formulation^[41]. When the formulation inverts, the viscosity of
436 the system increases significantly. The results showed that the liquid crystal gels had
437 pseudoplastic flow characteristics (shear thinning system) Viscosity increased at low
438 shear rate and decreased at high shear rate. One of the advantages of shear thinning
439 agents is that they have high viscosity during eye opening and stabilize tear film.
440 When the blink occurs, the gel becomes thinner to prevent the irritation produced by
441 the high viscosity Newtonian fluid^[42], so that the preparation is well distributed on the
442 surface of the eye.

443 Fig.7 (B) showed the relationship between the composite viscosity and the
444 angular frequency. The complex viscosity of the precursor formulations did not
445 change significantly with the angular frequency, but the complex viscosity of the
446 liquid crystal gel decreases with the increase of the angular frequency. These
447 situations were conducive to the uniform dispersion of the gels in the eye.

448 The experiment adopts the oscillation-frequency test mode. As exhibited in Fig.7
449 (C), the precursor preparations (F2 and F0) exhibits G'' (Viscous modulus) $>G'$ (Elastic
450 Modulus), and the viscous modulus was dominant, showing liquid-like behavior. At
451 the same time, the liquid-like behavior of the precursor formulations were more
452 conducive to the delivery of ophthalmic drugs. When the precursor formulations were
453 transformed into a hexagonal liquid crystal gel, the elastic modulus G' and the
454 viscosity modulus G'' are much higher than the formulations before the phase change.
455 Furthermore, after phase inversion to form the liquid crystal gels, G' increases with
456 increasing frequency, while G'' first rises and then decreases with increasing frequency.
457 However, in the entire scanning process, the values before and after G''' did not
458 change significantly. In the frequency range of 0.01-0.05Hz, the viscosity modulus
459 was dominant ($G'' > G'$), but in the frequency range of 0.05-10Hz, the elastic modulus
460 was dominant ($G' > G''$), It could be concluded that the external frequency changes

461 will affect the viscoelasticity of the liquid crystal gel, and we can infer that the liquid
 462 crystal gel had less irritation to the eyes at low frequencies^[43]. It could be concluded
 463 that the external frequency changes would affect the viscoelasticity of the liquid
 464 crystal gel, and we could deduce that the liquid crystal gel had less irritation to the
 465 eyes at low frequencies. At high frequencies, the preparations could resist the damage
 466 of high frequency blinking shear force and had good stability. Therefore, the "liquid"
 467 behavior of the precursor formulations were more conducive to the delivery of
 468 ophthalmic drugs. Besides, the gel-like behavior of liquid crystal gels could make the
 469 drug release slowly.

470 Fig.7 (D) described the effect of temperature on the formulations. Whether it was
 471 a precursor preparation or a liquid crystal gel, its viscosity would not change
 472 significantly with the increase of temperature, Besides, H5 was more stable than H0,
 473 indicating that PN could enhance the stability of the internal structure of liquid crystal
 474 gel and was suitable for ophthalmology medicine.



475
476
477
478
479
480
481
482
483
484
485
486
487
488
489
490

491

492

493 Fig.7 (A) Apparent shear viscosity as function shear rate of precursor preparations(F0
494 and F2) and H_{II} gels (H0 and H2). Inset exhibits the viscosity at specific shear rate
495 (0.10 1/s). (B) Complex viscosity of precursor preparations (F0 and F2) and H_{II} gels
496 (H0 and H2) at 37 °C as a function of the applied angular frequency. (C) Variation of
497 elastic modulus G' and viscous modulus G'' as a function of frequency for precursor
498 preparations (F0 and F2) and H_{II} gels (H0 and H2). (D) Temperature sweep results
499 displaying the complex viscosity of precursor preparations (F0 and F2) and H_{II} gels
500 (H0 and H2). (Strain: 0.5% Frequency: 1 Hz) from 25 °C to 45 °C.

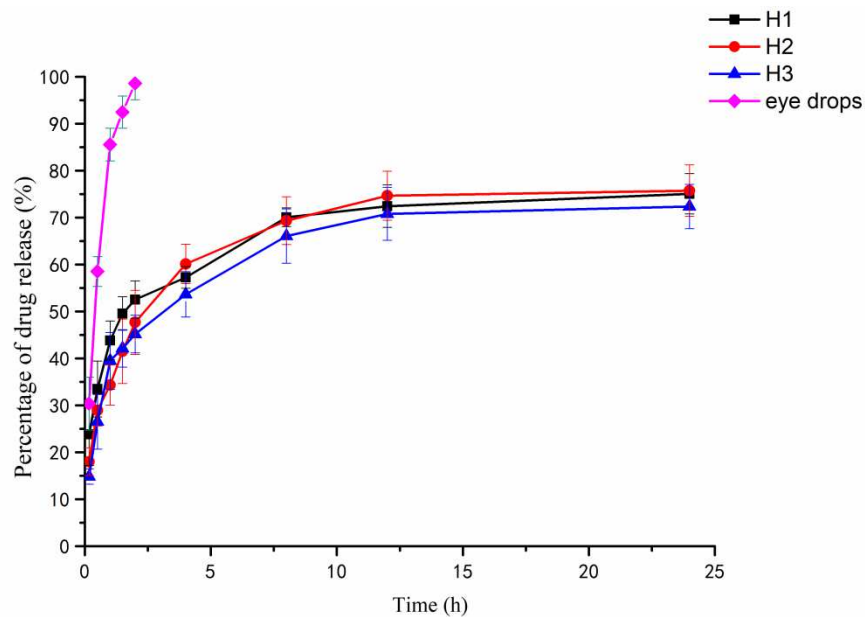
501

502 3.3 In vitro studies

503 3.3.1 In vitro release study

504 As shown in Fig.8, the Q_n of H1, H2, H3 in the previous hour were 43.84%,
505 34.31% and 39.49%. However, the Q_n of eye drops had reached 85.54%, and it had
506 reached 98.59% within two hours. Obviously, the drug release increased by
507 approximately 2-folds from eye drops in comparison to the corresponding H_{II} gels. It
508 could be speculated that H_{II} gels has a good sustained-release effect compared with
509 traditional eye drops.

510 Hydrophilic PN is located in the aqueous channels of H_{II} mesophase, and the
511 drug release rate is influenced by the lattice parameters and the diameter of water
512 cylinders. Therefore, we can deduce that although H3 contains the largest drug
513 loading, its lattice parameters and water channel diameters are smaller than those of
514 H1 and H2, which was supported by the outcomes of SAXS. The release trends of the
515 three drug loads were similar. However, in terms of cumulative release, H2 was
516 higher than H1 and H3. According to the above results, H2 has the best drug release
517 effect, and we will choose H2 for the following experiments.



518

519 Fig. 8. In vitro release curves of H_{II} gels and PN eye drops. All data reported as
 520 reported as mean values ± SD, (n=3).

521 As shown in Table 4, through the in vitro release data of liquid crystal gel, the
 522 regression coefficient of the Higuchi model was between 0.8420 and 0.8465, and was
 523 larger than other models, so it proved to be diffusion controlled release^[44]. The
 524 Ritger-Peppas model was used to evaluate the drug release mechanism. The ‘n’ of the
 525 three preparations was less than 0.45, so the drug was controlled by Fickian
 526 diffusion^[45].

527

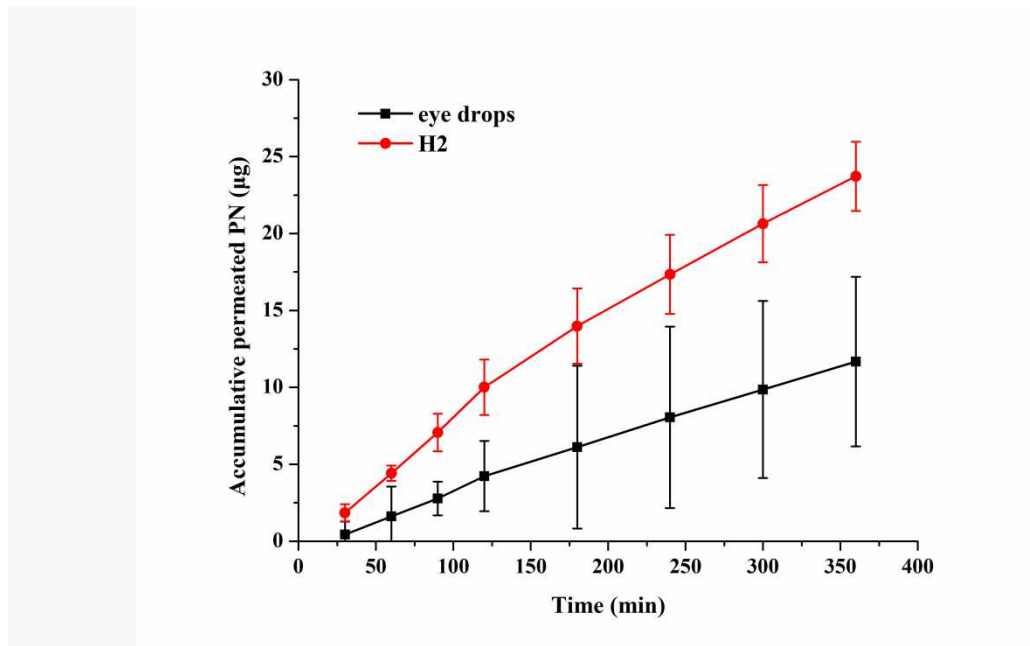
528 Table 4. Release kinetics of in situ hexagon liquid crystal and PN eye drops

529

Formulations	Zero-order	First-order	Higuchi	Ritger-Peppas	
	R ²	R ²	model R ²	R ²	n
H1	0.6941	0.7395	0.8432	0.9576	0.2366
H2	0.6331	0.7319	0.8465	0.9583	0.3024
H3	0.6324	0.7373	0.8420	0.9313	0.3151
Eye drops	0.3567	0.4330	0.5247	0.8041	0.0243

530

531 3.3.2 Study on corneal penetration



532 Fig.9 In vitro corneal permeability curve of HII gels and PN eye drops

533 Table 5. In vitro corneal osmotic parameters of in situ liquid crystal and PN eye drops

534 All the data are representative ($\bar{x} \pm SD, n = 3$)

535

536

537

538 Formulations	539 $J_{ss} \times 10^2 /$ ($\mu\text{g} \cdot \text{s}^{-1} \text{cm}^{-2}$)	540 $P_{app} \times 10^6 /$ ($\text{cm} \cdot \text{s}^{-1}$)
541 H2	542 $3.5 \pm 0.021^*$	$0.35 \pm 0.18^*$
543 Eye drops	0.055 ± 0.018	0.11 ± 0.15

544 *P < 0.05, which is statistically different from eye drops.

545 Fig.10 showed the corneal penetration curve of HII gel and eye drops. Obviously,

546 the corneal permeability of the liquid crystal gel group was higher than that eye drops

547 group. It could be seen from Table 5. that the apparent permeability coefficients of H2

548 and eye drops were 0.35×10^6 and 0.11×10^6 cm/s, respectively. Compared with

549 commercially available drugs, the apparent permeability coefficient of H2 was 3.19

550 times that of eye drops, indicating that the rabbit cornea penetrates much more PN

551 than eye drops.

552 First of all, we speculate that this difference may be due to the good

553 biocompatibility of biolipid carriers and corneal epithelial cells, which leads to

554 increased solubility of the drug, which makes it easier to penetrate the corneal
 555 barrier^[45]. Furthermore, many literatures demonstrated that PT can promote the
 556 transdermal absorption of hydrophilic drugs^[46]. Therefore, it is inferred that PT itself
 557 has permeability promoting properties and can enhance the permeability of the
 558 corneal epithelium^[47,48].

559 3.3.3 Corneal hydration level

560 By calculating the HL value to assess the tissue damage to the cornea. The HL
 561 value of a healthy cornea is between 76~80%, and the corneal hydration value
 562 exceeds 83%, indicating a certain degree of corneal damage. The HL value of the eye
 563 drops was higher than 80%, while the HL value of the H_{II} gels preparation was 76.91±
 564 0.43%. The results showed that the H_{II} gels would not produce obvious corneal
 565 irritation and damage.

566

567 4.4 In vivo study

568 4.4.1 Ocular irritation test

569 As shown in Table 6, after a single administration, the in situ liquid crystal and
 570 eye drops had little effect on the cornea and iris, the cornea was not turbid, and the
 571 conjunctiva was free of redness, congestion, swelling and other irritation. After
 572 repeated administration, the liquid crystal gel would be located in the subconjunctival
 573 sac of the rabbit's eye. The conjunctiva may be slightly reddened due to blinking
 574 reaction, but the score was lower than 3. The comprehensive results showed that both
 575 in situ liquid crystal and PN eye drops had less irritating to rabbit eyes.

576

577 Table 6. Evaluation results of ocular irritation in single and multiple doses of
 578 improved Draize test (n=6)

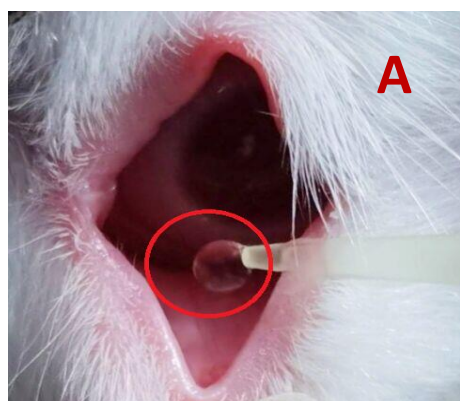
579

Location	Physiological saline		Eye drops		F5	
	Single	Long-term	Single	Long-term	Single	Long-term
Cornea	0	0	0	0	0	0
Iris	0	0	0	0	0	0

Conjunctival congestion	0	0	0.2	0.4	0	0.4
Conjunctival edema	0	0.5	0.1	0.2	0.3	1.2
Secretions	0	0	0.1	0	0	0
Sum score	0	0.5	0.4	0.6	0.3	1.6

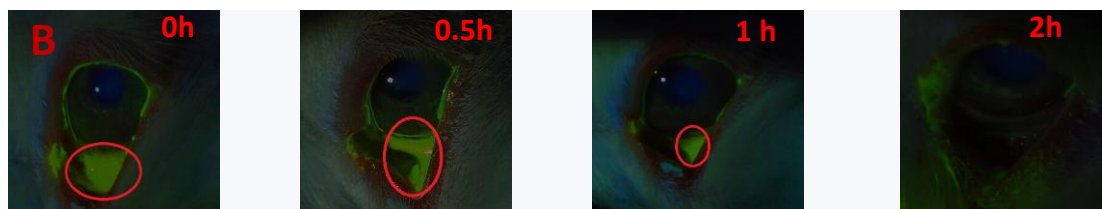
580

581 4.4.2 Pre-Corneal Residence Time Analysis



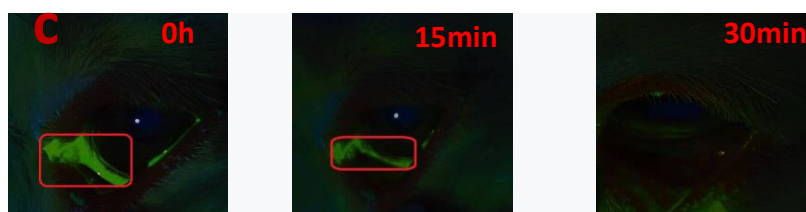
582

583



584

585



586

587

588 Fig.10. Pre-corneal distribution of administration of the formulations at specified time
589 points. (A) Anterior surface of eyeball, (B) H_{II} gel, (C) eye drops.

590 As displayed in Fig. 10, the H_{II} gel could observe a stronger fluorescence
591 intensity. Compared with eye drops, the fluorescent signal of the H_{II} gel was
592 distributed in the subconjunctival capsule for to 2 h. Obviously, the rabbit eyes coated

593 with eye drops did not show strong fluorescence intensity and were quickly cleared
594 after 30 min, which indicates that the retention time of eye drops in the eye was very
595 short. This showed that compared with traditional eye drops, H_{II} gel could significantly
596 increase the contact time of the drug in front of the cornea. We speculated that the
597 good bioadhesion of PT led to relatively strong fluorescence intensity and slow
598 clearance. Secondly, PT may interacted with the mucin in the corneal epithelium,
599 thereby shortening the residence time of the drug on the corneal surface^[49], or PT may
600 have a certain degree of biodegradability in the body, causing the fluorescence
601 intensity to gradually decrease over time. Generally, H_{II} gel has good bioadhesion and
602 would not reduce the residence time due to blinking, which has been verified by
603 previous rheological results.

604 5 Conclusion

605 In summary, compared with eye drops, the liquid crystal gel precursor
606 formulation significantly improves the bioavailability and biocompatibility of the
607 drug. The in vitro release test results show that the liquid crystal gel had a better
608 sustained-release effect, avoiding the shortcomings of repeated administration. In
609 vitro corneal penetration experiments showed that liquid crystal gel could enhance
610 corneal penetration. In addition, the corneal hydration level and Draize test proved
611 that the preparation was less irritating to the eyes and was suitable for ocular
612 administration. The analysis of the pre-corneal residence time proved that the
613 preparation has good bioadhesion. In short, the liquid crystal gel precursor
614 formulation had good fluidity and convenient administration. It had good bioadhesion,
615 sustained release, good corneal permeability and low irritation. The research results
616 provided a new way and method for the clinical treatment of glaucoma or other eye
617 diseases, and provide a theoretical basis and reference for other topical drug research.

618 Availability of data and material

619 The datasets used or analysed during the current study are available from the
620 corresponding author on reasonable request.

621

622 Declaration of interest

623 The authors declare that there is no conflict of interest.

624

625 **Funding Information**

626 The authors gratefully acknowledge support from the National Natural Science
627 Foundation of China (No.81803831), Key University natural science research project
628 of Anhui province (KJ2018A0301). and Anhui Provincial Talents Project for youth in
629 Universities (No.gxyq2018025).

630

631 **Acknowledgements**

632 The content is solely the responsibility of the authors and does not necessarily
633 represent the official views of Anhui University of Chinese Medicine.

634

635 **Conflict of interest**

636 The authors declared that they have no conflicts of interest to this work. We
637 declare that we do not have any commercial or associative interest that represents a
638 conflict of interest in connection with the work submitted.

639

640

641 **References**

- 642 [1] Li Q, Wang J, Shahani S, et al. Biodegradable and photocrosslinkable polyphosphoester
643 hydrogel. *Biomaterials*. 2006;27(7):1027-1034.
- 644 [2] Dong Y, Hassan WU, Kennedy R, et al. Performance of an in situ formed bioactive hydrogel
645 dressing from a PEG-based hyperbranched multifunctional copolymer. *Acta Biomater*.
646 2014;10(5):2076-2085.
- 647 [3] Nirmal H, Bakliwal S, Pawar S. In-situ gel: new trends in controlled and sustained drug
648 delivery system. *Int J PharTech Res*. 2010;2(2):1398-1408.
- 649 [4] Fakhari A, Corcoran M, Schwarz A. Thermogelling properties of purified poloxamer
650 407. *Heliyon*. 2017;3(8):e00390. Published 2017 Aug 30.
- 651 [5] Pereira G, Dimer F, Guterres S. Formulation and characterization of Poloxamer 407®:
652 thermoreversisble gel containing polymeric microparticles and hyaluronic acid. *Quim Nova*.
653 2013;36(8):1121–5.
- 654 [6] Wen-Di M, Wang C, Nie S, Pan W. Pluronuc F127-g-poly (acrylic acid) copolymers as in situ
655 gelling vehicle for ophthalmic drug delivery system. *Int J Pharm*. 2007;350:247–56.
- 656 [7] Edsman K, Carfors J, Petersson R. Rheological evaluation of polxamer as an in situ gel for
657 ophthalmic use. *Eur J Pharm Sci*. 1998;6:105–12.

658 [8] Phaechamud T, Mahadlek J. Solvent exchange-induced in situ forming gel comprising ethyl
659 cellulose-antimicrobial drugs. *Int J Pharm.* 2015;494(1):381-392.

660 [9] Narurkar MM, Mitra AK. Prodrugs of 5-iodo-2'-deoxyuridine for enhanced ocular
661 transport. *Pharm Res.* 1989;6(10):887-891.

662 [10] Srividya B, Cardoza R, Amin P . Sustained ophthalmic delivery of ofloxacin from a pH
663 triggered in situ gelling system. *J Control Release.* 2001;73:205-211.

664 [11] Wu H, Liu Z, Peng J, Li L, Li N, Li J, et al. Design and evaluation of baicalin-containing in
665 situ pH-triggered gelling system for sustained ophthalmic drug delivery. *Int J*
666 *Pharm.*2011;410:31-40.

667 [12] Jain SP, Shah SP, Rajadhyaksha NS, Singh P S PP, Amin PD. In situ ophthalmic gel of
668 ciprofloxacin hydrochloride for once a day sustained delivery. *Drug Dev Ind Pharm.*
669 2008;34(4):445-452

670 [13] Fan J, Liu F, Wang Z. Shear rheology and in-vitro release kinetic study of apigenin from
671 lyotropic liquid crystal. *Int J Pharm.* 2016;497(1-2):248-254.

672 [14] Mei L, Xie Y, Huang Y, et al. Injectable in situ forming gel based on lyotropic liquid crystal
673 for persistent postoperative analgesia. *Acta Biomater.* 2018;67:99-110.

674 [15] Quigley HA, Broman AT. The number of people with glaucoma worldwide in 2010 and 2020.
675 *Br J Ophthalmol.* 2006;90(3):262-267.

676 [16] Wei J, He HL, Zheng CL, Zhu JB. *Yao Xue Xue Bao.* 2011;46(8):990-996.

677 [17] Nair KL, Vidyanand S, James J, Kumar, et al. Pilocarpine-loaded poly (dl-lactic-co-glycolic
678 acid) nanoparticles as potential candidates for controlled drug delivery with enhanced ocular
679 pharmacological response. *J.Appl. Polym. Sci.* 2012;124 (3), 2030–2036.

680 [18] Aktaş Y, Unlü N, Orhan M, Irkeç M, Hincal AA. Influence of hydroxypropyl
681 beta-cyclodextrin on the corneal permeation of pilocarpine. *Drug Dev Ind Pharm.*
682 2003;29(2):223-230.

683 [19] Zimmerman TJ. Pilocarpine. *Ophthalmology.* 1981;88(1):85-88.

684 [20] Kao HJ, Lin HR, Lo YL, Yu SP. Characterization of pilocarpine-loaded chitosan/Carbopol
685 nanoparticles. *J Pharm Pharmacol.* 2006;58(2):179-186.

686 [21] Wang X, Zhang Y, Huang J, et al. Self-assembled hexagonal liquid crystalline gels as novel
687 ocular formulation with enhanced topical delivery of pilocarpine nitrate. *Int J Pharm.*
688 2019;562:31-41.

689 [22] Coscia BJ, Yelk J, Glaser MA, Gin DL, Feng X, Shirts MR. Understanding the Nanoscale
690 Structure of Inverted Hexagonal Phase Lyotropic Liquid Crystal Polymer Membranes. *J Phys*
691 *Chem B.* 2019;123(1):289-309.

692 [23] Xingqi W, Yong Z, Xing L, et al. Cubic and hexagonal liquid crystal gels for ocular delivery
693 with enhanced effect of pilocarpine nitrate on anti-glaucoma treatment. *Drug Deliv.*
694 2019;26(1):952-964.

695 [24] Zabara A, Mezzenga R. Controlling molecular transport and sustained drug release in
696 lipid-based liquid crystalline mesophases. *J Control Release.* 2014;188:31-43

697 [25] Chen YL, Gui SY, Liang X. Preparation and evaluation of intraarticular injectable
698 sinomenine hydrochloride-loaded in-situ liquid crystals. *Acta Pharm Sin.* 2016;51:132–139

699 [26] Qi, H., Chen, W., Huang, C., Li, L., Chen, C., Li, W., Wu, C., 2007. Development of
700 apoloxamer analogs/carbopol-based in situ gelling and mucoadhesive ophthalmic
701 delivery system for puerarin. *Int. J. Pharmaceut.* 337 (1), 178-187.

702 [27] Jie H, Liu L, Shuangying G, et al. A Novel Phytantriol-Based In Situ Liquid Crystal Gel for
703 Vaginal Delivery. *AAPS PharmSciTech*. 2019;20(5):185.

704 [28] Milak S, Zimmer A. Glycerol monooleate liquid crystalline phases used in drug delivery
705 systems. *Int J Pharm*. 2015;478(2):569-587.

706 [29] Chen Y, Liang X, Ma P, et al. Phytantriol-based in situ liquid crystals with long-term release
707 for intra-articular administration. *AAPS PharmSciTech*. 2015;16(4):846-854.

708 [30] Báez-Santos YM, Otte A, Mun EA, et al. Formulation and characterization of a liquid
709 crystalline hexagonal mesophase region of phosphatidylcholine, sorbitan monooleate, and
710 tocopherol acetate for sustained delivery of leuprolide acetate. *Int J Pharm*. 2016;514(1):314-321.

711 [31] Ye J, Wang Q, Zhou X, Zhang N. Injectable actarit-loaded solid lipid nanoparticles as passive
712 targeting therapeutic agents for rheumatoid arthritis. *Int J Pharm*. 2008;352(1-2):273-279.

713 [32] Wang X, Zhang Y, Huang J, et al. A Novel Phytantriol-Based Lyotropic Liquid Crystalline
714 Gel for Efficient Ophthalmic Delivery of Pilocarpine Nitrate. *AAPS PharmSciTech*.
715 2019;20(1):32. Published 2019 Jan 2.

716 [33] Moustafa MA, El-Refaie WM, Elnaggar YSR, Abdallah OY. Gel in core carbosomes as novel
717 ophthalmic vehicles with enhanced corneal permeation and residence. *Int J Pharm*.
718 2018;546(1-2):166-175.

719 [34] Yu S, Wang QM, Wang X, et al. Liposome incorporated ion sensitive in situ gels for
720 ophthalmic delivery of timolol maleate. *Int J Pharm*. 2015;480(1-2):128-136.

721 [35] Bhatta RS, Chandasana H, Chhonker YS, et al. Mucoadhesive nanoparticles for prolonged
722 ocular delivery of natamycin: In vitro and pharmacokinetics studies. *Int J Pharm*.
723 2012;432(1-2):105-112.

724 [36] Fiscella R G . *Ophthalmic Drug Formulations - ScienceDirect[J]*. *Clinical Ocular*
725 *Pharmacology (Fifth Edition)*, 2008:17-37.

726 [37] Phan S, Fong WK, Kirby N, Hanley T, Boyd BJ. Evaluating the link between self-assembled
727 mesophase structure and drug release. *Int J Pharm*. 2011;421(1):176-182.

728 [38] Fong WK, Hanley T, Boyd BJ. Stimuli responsive liquid crystals provide 'on-demand' drug
729 delivery in vitro and in vivo. *J Control Release*. 2009;135(3):218-226.

730 [39] Amar-Yuli I, Garti N. Transitions induced by solubilized fat into reverse hexagonal
731 mesophases. *Colloids Surf B Biointerfaces*. 2005;43(2):72-82.

732 [40] Chang CM, Bodmeier R. Swelling of and drug release from monoglyceride-based drug
733 delivery systems. *J Pharm Sci*. 1997;86(6):747-752.

734 [41] Wang B, Huang Y, Huang Z, et al. Self-assembling in situ gel based on lyotropic liquid
735 crystals containing VEGF for tissue regeneration. *Acta Biomater*. 2019;99:84-99.

736 [42] Mezzenga R, Meyer C, Servais C, Romoscanu AI, Sagalowicz L, Hayward RC. Shear
737 rheology of lyotropic liquid crystals: a case study. *Langmuir*. 2005;21(8):3322-3333.

738 [43] Wan J, Wang SM, Gui ZP, et al. Phytantriol-based lyotropic liquid crystal as a transdermal
739 delivery system. *Eur J Pharm Sci*. 2018;125:93-101.

740 [44] Elgindy NA, Mehanna MM, Mohyeldin SM. Self-assembled nano-architecture liquid crystalline
741 particles as a promising carrier for progesterone transdermal delivery. *Int J Pharm*.
742 2016;501(1-2):167-179.

743 [45] Unagolla JM, Jayasuriya AC. Drug transport mechanisms and in vitro release kinetics of
744 vancomycin encapsulated chitosan-alginate polyelectrolyte microparticles as a controlled drug delivery
745 system. *Eur J Pharm Sci*. 2018;114:199-209.

746 [46] Chu XQ, Huang J, Li ZG, et al. On the Structure and Transdermal Profile of Liquid Crystals
747 Based on Phytantriol. *Curr Drug Deliv.* 2018;15(10):1439-1448.

748 [47] Agibayeva LE, Kaldybekov DB, Porfiryeva NN, et al. Gellan gum and its methacrylated
749 derivatives as in situ gelling mucoadhesive formulations of pilocarpine: In vitro and in vivo
750 studies. *Int J Pharm.* 2020;577:119093.

751 [48] Destruel PL, Zeng N, Seguin J, et al. Novel in situ gelling ophthalmic drug delivery system
752 based on gellan gum and hydroxyethylcellulose: Innovative rheological characterization, in vitro
753 and in vivo evidence of a sustained precorneal retention time. *Int J Pharm.* 2020;574:118734.

754 [49] Zhao R, Li J, Wang J, Yin Z, Zhu Y, Liu W. Development of Timolol-Loaded Galactosylated
755 Chitosan Nanoparticles and Evaluation of Their Potential for Ocular Drug Delivery. *AAPS*
756 *PharmSciTech.* 2017;18(4):997-1008.

757

758